Macromolecules

ARTICLE

pubs.acs.org/Macromolecules

# New Insights into Ionic Aggregate Morphology in Zn-Neutralized Sulfonated Polystyrene Ionomers by Transmission Electron Tomography

Florent Dalmas* and Eric Leroy

ICMPE (Institut de Chimie et des Matériaux Paris-Est), Equipe "Systèmes Polymères Complexes", UMR 7182 CNRS/Université Paris-Est Créteil, 2-8 rue Henri Dunant, 94320 Thiais, France

Supporting Information

**ABSTRACT:** The three-dimensional microstructure of ionic aggregates in Zn-neutralized sulfonated polystyrene ionomers was characterized, for the first time, by transmission electron tomography. Two methods were used in order to prepare ionomer films: the hot-pressing and solvent-casting. With the first method, spherical aggregates with a mean diameter of about 5 nm are observed within the material. They are heterogeneously dispersed within the matrix and tend to form a network. When the second processing method is used, a nanoplatelet shape (with a thickness of about 6 nm) is unambiguously observed for the ionic aggregates. A preferential alignment of these aggregates parallel to the film plane is induced by this method. The solvent-casting process is a very slow method where the medium viscosity is gradually increasing; such an aggregate morphology is assumed to represent a complete aggregation state for the ionic groups.

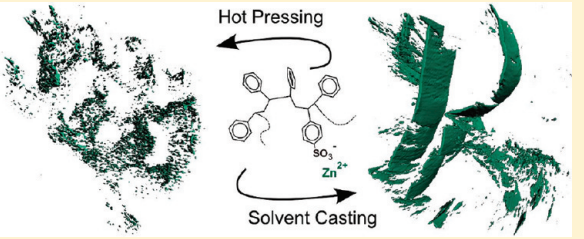


## 1. INTRODUCTION

Ionomers are defined as polymer chains on which a small amount of ionic pairs are grafted. They have been widely studied in the past 30 years[1] since they exhibit unexpected thermomechanical properties.[2−5] The appearance of a long rubbery plateau with a high elastic modulus is usually observed in a temperature range located above the polymer glass transition temperature. Moreover, two main features of interest have been highlighted in ionomers: the formation of a complex microstructure of ionic aggregates within the materials and a physical cross-linking effect induced by interchain ionic interactions.[3,6−8] Such cross-linking nodes are reversible by thermal activation and confer thermoplastic properties to the ionomers in contrast to chemically cross-linked polymers. These novel mechanical properties are directly related to the chemical structure of the macromolecules and the nature of the ionic pairs[9,10] as well as to the processing route for the materials. In particular, previous works have shown that the final microstructure of the ionic aggregates in sulfonated polystyrene (SPS) ionomers is strongly dependent on the sulfonation level, polydispersity of the polymer, and processing conditions.[11−13] For instance, a rapid solvent evaporation rate in casted films of a Zn-neutralized SPS (SPS-Zn) ionomer with an ionic content of about 3.4 mol % leads to spherical aggregates of about 3 nm in diameter,[12] while a SPS-Zn with a sulfonation degree of 5.3 mol % prepared by compression-molding induces two coexisting shapes for the ionic aggregates as solid spheres (diameter of about 5 nm) and shells or vesicles (diameter from 12 to 34 nm), respectively.[11]

Despite the abundant literature on ionomers, relationships between processing conditions and microstructure (i.e., the morphology and dispersion of the ionic aggregates) are far from being completely understood. It is assumed in this contribution that a better understanding of these relationships could be achieved by exploiting recent advances in transmission electron microscopy (TEM) that provide new powerful tools for the observation of nanostructured materials. Although the first paper using tomography techniques in TEM in order to study polymeric materials was published as early as 1988 by Spontak et al.,[14] electron tomography recently emerged as an efficient tool to get a detailed and realistic description of nanostructured polymeric systems.[15−22] Conventional TEM only provides two-dimensional (2D) projections of a three-dimensional (3D) sample of a given thickness. As a consequence of these limitations, the interpretation of such images is not unambiguous. On the contrary, TEM tomography (TEMT) generates 3D images with a nanometer scale resolution from tilt series of 2D projections.[23] For instance, substantial further progresses on the microstructural analysis of block copolymers[24,25] or polymeric nanocomposites[16−18,21,22] have been achieved during the past decade by this technique. Thus, TEMT constitutes a meaningful alternative way for the morphological analysis of complex polymeric nanostructures that has so far never been applied to ionomers.

In the present study, three-dimensional electron tomography observations were carried out on model ionomer systems based on Zn-neutralized randomly sulfonated polystyrene, using two

**Received:** July 25, 2011
**Revised:** September 20, 2011
**Published:** September 29, 2011

different conditions to prepare ionomer films: solution-casting and hot-pressing.

## 2. EXPERIMENTAL SECTION

**2.1. Materials.** Atactic polystyrene (PS) was purchased from Tebubio ($M_w = 180 \times 10^3$, $M_w/M_n = 2.5$). Purity of the PS was checked by SEC (size exclusion chromatography) and NMR (nuclear magnetic resonance). Randomly sulfonated polystyrene (SPS) was prepared by solution sulfonation of PS in dichloromethane using sulfate acetyl as sulfonation agent according to the procedure described by Makowski et al.[26] and elsewhere.[27] A sulfonation degree of about 3 mol % was measured by titration with methanolic NaOH. SPS-Zn was prepared by adding a methanolic solution of zinc acetate dropwise to a stirred 10% (w:v) solution of SPS (in a 9:1 (v:v) toluene/methanol mixture). The resulting solution was stirred for 3 h at 40−50 °C and finally precipitated and washed with methanol. The ionomer was recovered by filtration and dried under vacuum for 12 h at 70 °C.

Ionomer films (with a thickness of about 300 $\mu$m) were prepared using two methods. In the first method (referred to as the C (for casted) method in the text), a SPS-Zn film was processed by casting a 10% (w:v) solution of SPS-Zn in a 9:1 (v:v) toluene/methanol mixture. The clear solution was cast in a Teflon mold, and heated at 50 °C for 24 h, until most of the solvent was evaporated. An as-cast specimen was further dried under vacuum, using a temperature ramp from 50 to 140 °C, with 5 h isothermal steps after every 10 °C increase. The sample was finally maintained at 140 °C for 17 h and cooled down very slowly to room temperature, with a cooling rate of about 0.5 °C $min^{-1}$. In a second method (referred to as the HP (for hot-pressed) method in the text), the raw SPS-Zn powder obtained at the end of the sulfonation step was pressed for 5 min at 200 °C under 0.5 MPa.

**2.2. Transmission Electron Tomography (TEMT).** Both films were microtomed at room temperature using a Leica Ultracut UCT microtome with a diamond knife at a cutting speed of 0.2 mm $s^{-1}$. The thin sections, of about 100 nm thickness, were floated onto deionized water and collected on a 400-mesh copper grid.

Tilt series were acquired using a FEI Tecnai F20 field emission gun transmission electron microscope operating at an accelerating voltage of 200 kV. 121 images were recorded with tilt angles ranging from −60° to +60° with an increment of 1°, using an Orius CCD Camera from Gatan. The pixel size of the projection was between 0.2 and 0.6 nm, depending on the observed sample. The exposure time for each projection was set to 0.4 s. Tilt series were acquired using the Digital Micrograph software (from Gatan), which allows for an automated acquisition with drift and focus correction (by cross-correlation) between each projection. The acquisition time of tilt series can reach 30 min. The overall electron dose received by the sample becomes critical and degradation of the sample may occur. In order to prevent significant degradation of the polymer, samples were maintained at −170 °C during the acquisition of the tilt series. The 914 high tilt liquid nitrogen cryogenic tomography specimen holder from Gatan was used.

Alignment and reconstruction were performed using the DigiECT software from DigiSENS. Alignment of the tilt series was realized with the seed-tracking procedure implemented in DigiECT. About 20 contrasted seeds, consisting in well-defined details from the sample microstructure, were automatically detected and tracked over the entire tilt series. In addition to the projection alignment, this procedure allows for the positioning of the tilt axis in the series. The SIRT reconstruction algorithm was used (Simultaneous Iterative Reconstruction Technique), with 15 iterations which is a good compromise between a high spatial resolution in the reconstructed volume and computation time.[28] Visualization of the volume was performed by surface-rendering after selecting an intensity level sufficient to enable the visualization of the objects.

The ImageJ software[29] was used for additional image analyses such as extraction of 2D slices from the reconstructed volumes and quantification of the objects by the "3D object counter" plug-in.[30]

## 3. RESULTS AND DISCUSSION

A Zn-neutralized sulfonated polystyrene was selected as a model ionomer in the present study as it is easy to prepare from polystyrene with a well-controlled sulfonation degree[26] and can be processed using various methods as compression-molding[5,7,9,11] or solvent-casting.[12,27,31] In addition, many structural investigations by various techniques are available in the literature for this polymeric materials. A wide range of microstructures have been previously observed in these corresponding materials by SAXS (small-angle X-ray scattering) or TEM and found to be strongly dependent on the processing method. In this paper, two methods were used in order to prepare films from the raw precipitated ionomer powders: the solvent-casting and hot-pressing. The first method is a very slow process where the medium viscosity is initially low and gradually increases; in contrast, the second method is faster but has a much higher initial viscosity. As a consequence, they open access to quite different kinetic and dynamic characteristics for the ionomer chains during the process and should accordingly lead to contrasting microstructures (shape, size, and dispersion of the ionic aggregates). A detailed description of processing conditions and sample preparation by ultramicrotomy is provided in the Experimental Section.

In a first step, microtomed films were investigated by TEM under defocus conditions (Figure 1). Taking advantage of the Z contrast between Zn cations ($Z = 30$) and the polymer matrix, TEM is indeed a suitable technique to observe ionic aggregates within ionomers and to analyze their microstructure.[6,8,11,12] Moreover, slight underfocus conditions (an optimized defocus of −2 $\mu$m was set in the present study) are commonly used when imaging polymeric systems or acquiring tilt series for 3D reconstruction.[16,22] By inducing phase contrast, such conditions provide a better contrast by enhancing the edge of the objects. Dark domains corresponding to Zn-rich aggregates relative to the PS matrix can be observed. For the HP SPS-Zn film, small aggregates with a typical length scale of about 5 nm and an aspect ratio close to 1 are observed in Figure 1a. From the absence of rodlike or disklike projections, we can assume that the aggregates are approximatively spherical. Such morphology for ionic aggregates is consistent with what was formerly observed in the literature for lightly sulfonated SPS-Zn ionomers prepared by compression molding or rapid casting.[7,12] These aggregates appear heterogeneously dispersed within the polystyrene matrix and tend to form a network. In contrast, and as already described in a previous study,[27] the morphology of the ionic aggregates is quite different in the C SPS-Zn film. The shape of the ionic aggregates appears to be strongly anisotropic, with nanoscopic rodlike structures about 5−10 nm thick and 50−100 nm long observed in Figure 1b. These observations suggest that those ionic aggregates are heterogeneously dispersed within the matrix as a 3D network. The words "appear" and "suggest" are used in the previous two sentences because one has to keep in mind that TEM images result from a two-dimensional projection of a 3D microstructure. Therefore, no unambiguous conclusions can be drawn from these experiments regarding the morphology of the aggregates, nanoplatelets, or rods. For instance, the image in Figure 1b is very similar to what can be observed in clay nanoplatelets filled

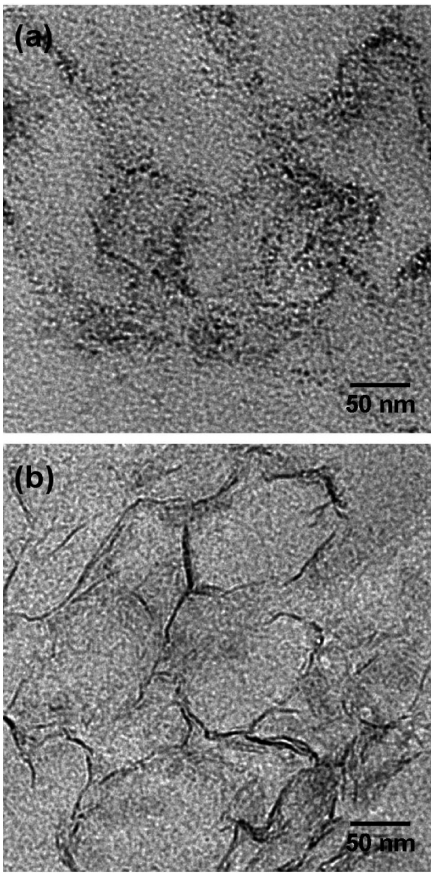


**Figure 1.** TEM images of the Zn-neutralized sulfonated polystyrene ionomer (SPS-Zn) prepared by (a) hot-pressing and (b) solution casting. See Experimental Section for further details on processing methods.

polymers[32] or in polymeric nanocomposites filled with rodlike silicate.[33]

From these observations a preliminary conclusion can be drawn that nanoscopic aggregates can be observed for both ionomer systems but that their shape and size differ. When the ionomer is hot-pressed after a rapid precipitation, the $SO_3^-/Zn^{2+}/SO_3^-$ triplets seem not to have sufficient time to aggregate in domains as large as those observed when the ionomer film is prepared by slow evaporation.

As a result, tomographic analysis was carried out on the same samples. Bright field tilt series in underfocus were acquired over a $\pm$ 60° tilt angle range with 1° steps. Figure 2a displays the volume-rendered image of the HP SPS-Zn film after surface-rendering with a threshold set so that the polymer matrix becomes transparent. In order to analyze the 3D microstructure in more details, orthogonal cross sections of this volume are also shown in Figure 2b. A better contrast is obtained in such digital slices than in conventional TEM, helping considerably in the analysis of the spatial organization of the ionic aggregates. Thus, ionic aggregates can be observed in Figure 2 with an almost spherical shape (typical diameter of 5 nm), heterogeneously dispersed within the polystyrene matrix. These aggregates are arranged in larger domains consisting in a long chain of "primary" spherical aggregates in the $x-y$ plane arranged in a more isotropic way in the $z$ direction.

One has to keep in mind when analyzing the data that a missing wedge in tilt series is responsible for a loss of resolution in the reconstructed volume in the direction parallel to the electron beam, i.e., the z direction corresponding to the sample thickness.[23] The resolution along the $y$ axis (parallel to the tilt axis), $d_y$, is solely limited by the projection resolution: $d_y$ = 0.6 nm. Then, as concluded by Midgley et al.,[23] the resolution in the other perpendicular directions is controlled by the sampling parameters (the sample thickness, the tilt angle range, and the number of projections). Using traditional mathematical treatments,[23] we can estimate $d_x$ = 1.6 nm and $d_z$ = 2.5 nm. It results in the artificially elongated shape observed for the ionic aggregates as can be observed in Figure 3, which details the orthogonal view of an ionic aggregate from the reconstructed volume of the HP SPS-Zn material. By assuming a spherical shape for the ionic aggregates in Figure 3, one can measure the apparent "elongation ratio" by calculating the ratio between the length of the aggregate measured in the $y-z$ plane and its diameter in the $x-y$ plane. A value of 2.1 is found, slightly higher than the value of 1.6 predicted by the theoretical criteria of Midgley et al.[23] Missing wedge problem can be solved by tilting the specimen up to 90°. This has been recently achieved by Kawase et al.,[34] who developed novel sample design and improved the specimen holder. In this case, no anisotropy in the resolution was found by the authors.

The size distribution of ionic aggregates was quantitatively evaluated. This was done by using the "3D object counter" plug-in[30] from ImageJ (with takes into account the connectivity of the objects in the three directions) after a basic image segmentation consisting in a median filter in the 3 × 3 pixel neighborhood followed by a binarization and a 3D opening filter (in order to remove "bridges" and small particles). The "white edge effect" resulting from the underfocus conditions used for tilt-series acquisition can be multiplied during the volume reconstruction (as it can be observed in Figures 2 and 5). Thus, only black objects were considered for image processing and 3D quantification, avoiding any overestimation of the apparent object size. Figure 4 presents the result of such an analysis on a 2D digital slice (Figure 4a) extracted from the reconstructed volume. The individual aggregates are shown in Figure 4b. About 700 aggregates were analyzed from two volume reconstructions. A total volume fraction of ionic aggregates of 2 vol % was found for the reconstructed volume. The resulting distribution of the aggregate volume is presented in Figure 4c. The size of most ionic aggregates (accounting to ~70 vol %) can be fitted according to a log-normal distribution with a mean volume of 63 $nm^3$ and a standard deviation of 0.5. This corresponds to a spherical shape for the aggregates with a mean radius of about 2.5 nm. Such morphology and size for ionic aggregates in SPS-Zn ionomer is in complete agreement with what have been observed for similar materials by SAXS or other imaging techniques such as STEM (scanning transmission electron microscopy).[3,6−8,11−13] Experimental determination of the above volume distribution is a challenging issue for which very few solutions are available. For instance, Batra et al. have recently proposed a simple approach to estimate the aggregation number in Zn-neutralized poly(dimethylsiloxane) (PDMS) ionomers from TEM observations by using data (density and formula weight) from a typical zinc salt.[35] As shown in this study, electron tomographic analyses present the major advantage of providing a direct measurement of the object volume without any assumption on the sample thickness. As a result, further analysis can be performed. For instance, if we assume that a zinc sulfonate triplet ($SO_3^-/Zn^{2+}/SO_3^-$) in the SPS-Zn ionomer is constituted by nine atoms and

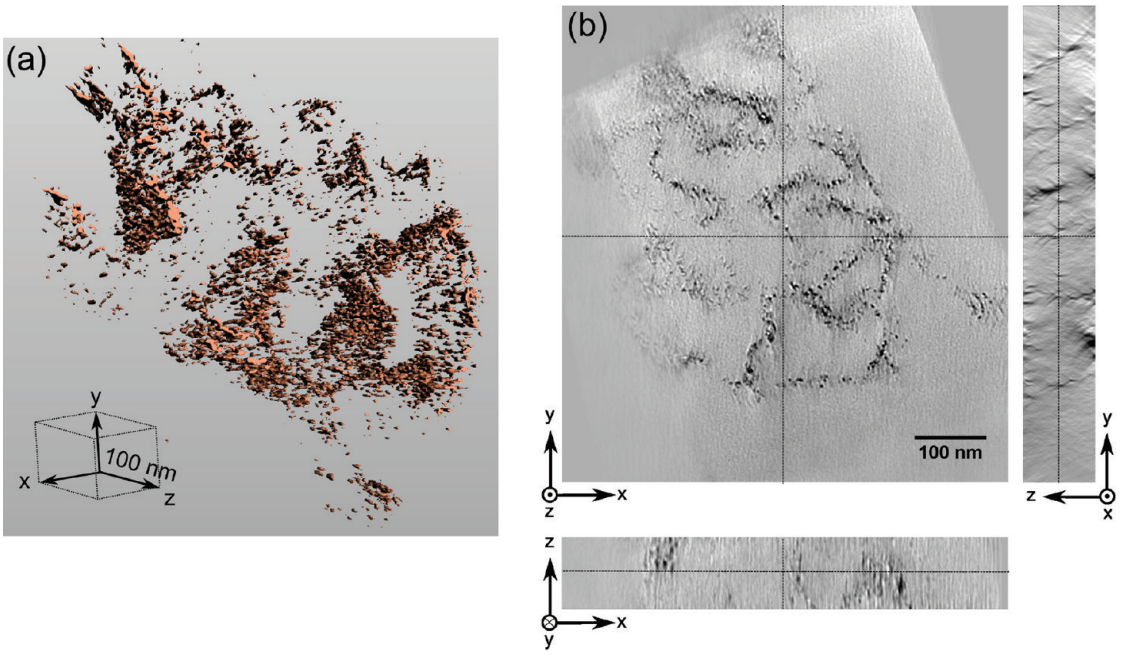


**Figure 2.** (a) 3D Reconstruction of the HP SPS-Zn material after surface-rendering of the Zn-rich phase. (b) Corresponding digital orthogonal slice images: the *z*-axis is the direction of the electron beam and also of the sample thickness. The dashed lines in each slice indicate the position of the other two orthogonal sections (a video file of the volume reconstruction is available as Supporting Information).

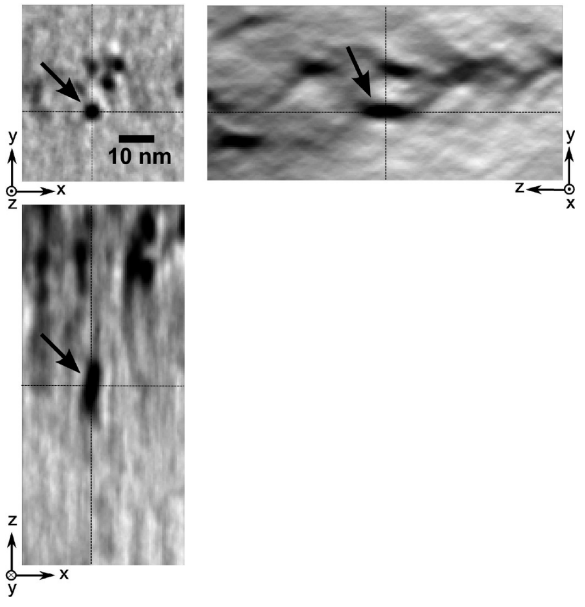


**Figure 3.** Digital orthogonal slice images extracted from the reconstructed volume of the HP SPS-Zn film: detail of a Zn-rich aggregate indicated by a black arrow.

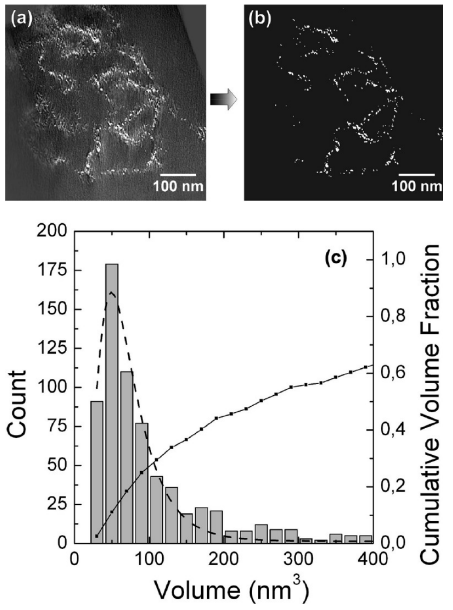


**Figure 4.** (a) Inverted digital slice from the reconstructed volume of the HP SPS-Zn film. (b) Corresponding binary image obtained after 3D particle analysis. (c) Volume distribution obtained on the segmented images. The dashed line corresponds to the best fit obtain with a log-normal law.

that an ionic aggregate is as dense as the zinc sulfonate salt (i.e., that only zinc sulfonate triplets reside inside the aggregate), aggregates with an average volume of 63 $nm^3$ as determined imply an aggregation number of 554 cations per aggregate. Nevertheless, such an aggregation number seems very high, and it is sterically impossible to have 554 cations connected to polymer chains within a single aggregate, suggesting that aggregates contain segments of polymer backbone.

The heterogeneous dispersion of the ionic aggregates as observed in Figure 2 was unexpected as it had never been observed, nor proposed before. This novel microstructure could be related to the broad molecular weight distribution of the polystyrene ($M_w/M_n$ = 2.5) used for the ionomer preparation by random sulfonation. Indeed, $^{23}$Na NMR studies[36] and synchrotron SAXS analyses[37] on Na-neutralyzed SPS ionomers (SPS-Na) have shown

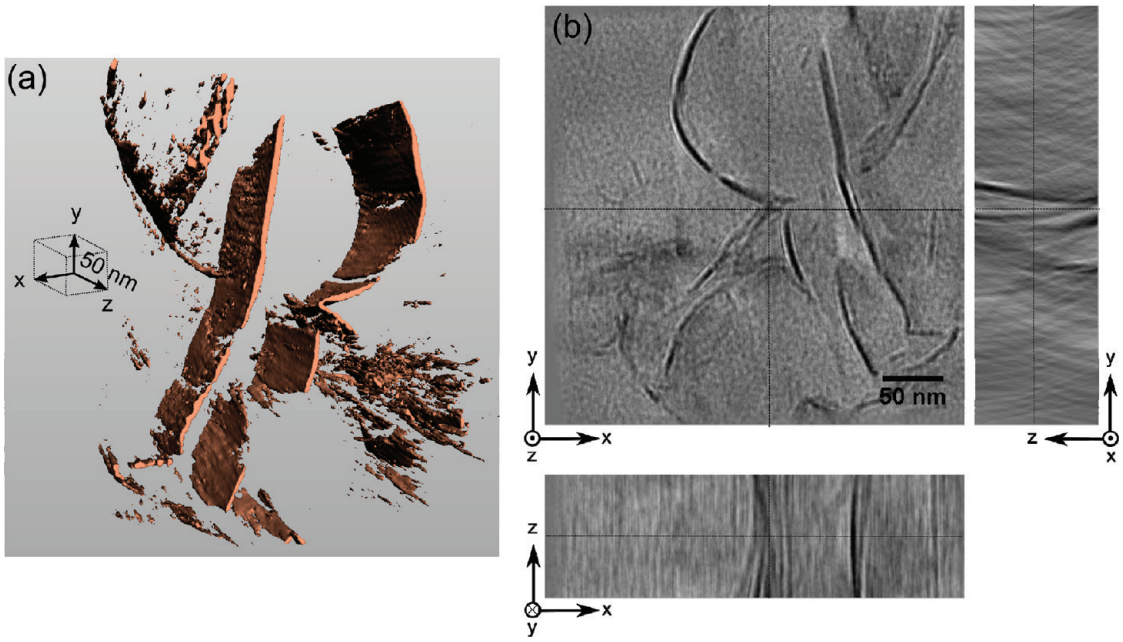


**Figure 5.** (a) 3D Reconstruction of the C SPS-Zn material after surface-rendering of the Zn-rich phase. (b) Corresponding digital orthogonal slice images (a video file of the volume reconstruction is available as Supporting Information).

that in polydisperse SPS-Na the lower molecular weight chains can disrupt some of the large aggregates. More isolated (i.e., nonaggregated) ions have also been observed by NMR as expected. The authors of this study suggested that the greater chain uniformity of the monodisperse ionomers limits the plasticization of the aggregates by low molecular weight components and allows for a more complete aggregation. Moreover, Batra et al.[35] have also observed that in PDMS ionomers the aggregate morphology is related to the chain length. With a similar number of ions per chain, large and anisotropic (rodlike shape) ionic aggregates have been observed for annealed ionomers with higher molecular weights, whereas smaller spherical aggregates have been found in low molecular weight ionomers.

In summary, SPS-Zn forms spherical ionic aggregates with a typical diameter of about 5 nm. It is speculated that because of the broad molecular weight distribution of the polystyrene backbone, some of these aggregates are disrupted and some aggregate-free areas are formed (even though some small multiplets with low aggregation number or isolated ions may remain, the present TEM technique being unable to observe them because of the low contrast). Higher molecular weight chains would contribute to the formation of more anisotropic aggregates, probably because of steric hindrance and higher intermolecular interactions, leading to the novel "network" dispersion observed for the aggregates in Figure 2.

Figure 5 displays the reconstructed volume obtained on the C SPS-Zn film prepared by solution casting, the tilt axis being still parallel to the *y*-axis. Very large ionic aggregates dispersed within the polymer matrix can be observed in the surface-rendering from Figure 5a highlighting the Zn-rich areas. These aggregates present a nanoplatelet shape with a thickness of about few nanometers, length a hundred of nanometers, and at least as wide as the sample is thick (as deduced from Figure 5b where some aggregates seem to cross the sample thickness). Sugimori et al.[25] have shown that TEMT failed to reconstruct part of 1D nano-objects (cylindrical nanodomains in block copolymers) whose orientation had a certain relationship with the tilt axis. However, such an artifact appeared limited in the case of 2D nanodomains as in clay nanoplatelets filled polymers even though some of the platelets may not be properly imaged in the 3D reconstruction.[16,19] As a result, one can directly compare the resulting microstructure from Figure 5 to what can be observed in this type of nanocomposite. Moreover, it is noteworthy to note in the orthogonal views (Figure 5b) that these aggregates appear aligned along the *z* direction. In TEM observations, the $x-y$ plane corresponds to the section of the film and the *z* direction is parallel to the film plane. Thus, we can conclude from the above observations that the solvent evaporation induces the formation of large anisotropic aggregates preferentially oriented along the plane of the film. This novel microstructure could be explained by the very slow solvent evaporation used for the solvent-casting film processing. Such a slow process allows the $SO_3^-/Zn^{2+}/SO_3^-$ triplets to aggregate in long platelets. Here again, an heterogeneous dispersion of the aggregates is observed, and as discussed before in the case of the HP SPS-Zn film, it could be related to the high polydispersity of the PS chains.

Moreover, these anisotropic aggregates have a thickness of the same order of magnitude as the diameter of the spherical aggregates previously observed in the HP SPS-Zn sample. Figure 6 illustrates the measurement of an aggregate thickness by considering the width at half-height of the intensity peak across the aggregate in order to avoid taking into account the white edges resulting from the underfocus and to not overestimate the thickness of the aggregate. A thickness of about 6 nm was found in complete agreement with the mean radius determined for the spherical aggregates in Figure 4 for the HP SPS-Zn film. Consequently, one can assume that the platelet shape corresponds to a complete state of ionic aggregation between the SPS-Zn chains that can be achieved during the slow processing method employed for the C SPS-Zn film. It is worth noting that this progressive organization in platelets is compatible with

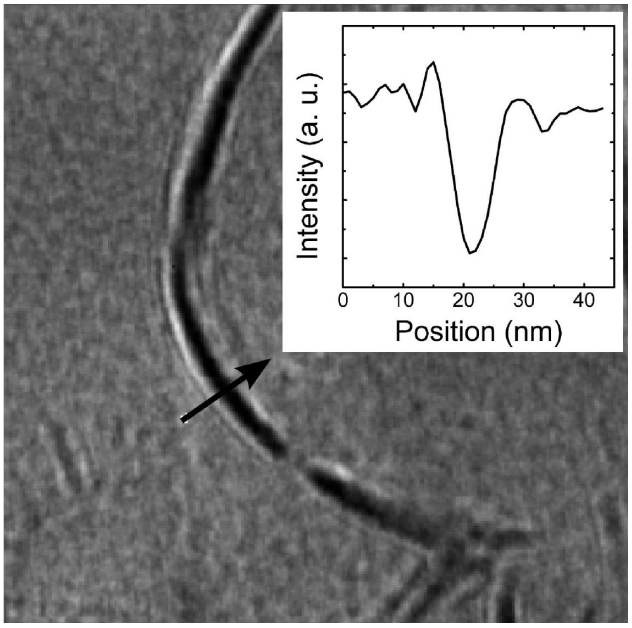


**Figure 6.** Details of the digital slice extracted from Figure 5b and the corresponding intensity line profile (inset) along the indicated arrow crossing an aggregate.

the "simple" 2D images of Figure 2, the evolution from Figure 2a to Figure 2b being already "predictable", but not fully evidenced.

## 4. CONCLUSIONS

The interpretation of 2D TEM images can be complicated because of projection problems. The use of electron tomography in the study of ionomers provides access for the first time, to the third dimension in TEM samples, thus eliminating any ambiguity in microstructural interpretation and allowing for a complete description of the morphology and dispersion of ionic aggregates. Depending on the processing method, two types of microstructure have been observed by this technique in SPS-Zn ionomers. When the material is hot-pressed, spherical aggregates (with a diameter of about 5 nm) are heterogeneously dispersed in the material. In contrast, when prepared by solvent casting, the ionomer present a microstructure consisting in much larger ionic aggregates. The important contribution of the 3D electron tomography in the present study is that one can unambiguously distinguish the platelet shape of these ionic aggregates (with a thickness of about 6 nm) and their preferential alignment parallel to the plane of the film.

As a result, the obtained microstructures for the two samples of SPS-Zn ionomers investigated in this study suggest that the system viscosity during processing plays a major role in the structuration process. The ionic group and polymer chain mobility during processing should probably affect the extent of aggregation achieved. One can assume that after a very slow solvent-casting process where the medium viscosity is gradually increasing from the solution to the solid state, large nanoplatelet aggregates have time to be formed, whereas when a fast processing method such as the hot-pressing is used, small spherical aggregates are created within the material with a diameter in the same order of magnitude of the platelet thickness. Nevertheless, the novel platelet structure and heterogeneous dispersion observed for the ionic aggregates in this study are not fully explained. One can speculate that they are related to the chemical characteristics of the polystyrene backbone (high average molecular weight and broad molecular weight distribution).

This study has highlighted the robustness and the effectiveness of transmission electron tomography in the analysis of ionomer microstructure. Further studies must be conducted on model ionomer systems with well-controlled chemical characteristics (e.g., molecular weight, polydispersity, nature of the cations, etc.) and processing conditions in order to get a comprehensive view of the structuration process in such materials.

## ■ ASSOCIATED CONTENT

**Supporting Information.** Movies showing the volume reconstruction for both ionomer films: HP SPS-Zn and C SPS-Zn. This material is available free of charge via the Internet at http://pubs.acs.org.

## ■ AUTHOR INFORMATION

### Corresponding Author

*Tel +33 1 49 78 12 86, Fax +33 1 49 78 12 08, e-mail dalmas@icmpe.cnrs.fr.

## ■ ACKNOWLEDGMENT

The authors are very grateful to J. Penelle for his fruitful comments. They thank J.-F. Vonet and S. Randriamahefa for the ionomer synthesis. They also acknowledge C. Achille for his contribution to some experimental data.

## ■ REFERENCES

(1) Eisenberg, A.; Kim, J. S. *Introduction to Ionomers*; Wiley-Interscience: New York, 1998; p 327.
(2) Hara, M.; Jar, P.; Sauer, J. A. *Polymer* **1991**, *32*, 1622.
(3) Hird, B.; Eisenberg, A. *Macromolecules* **1992**, *25*, 6466.
(4) Kim, J.-S.; Hong, M.-C.; Nah, Y. H. *Macromolecules* **2002**, *35*, 155–160.
(5) Weiss, R. A.; Yu, W.-C. *Macromolecules* **2007**, *40*, 3640–3643.
(6) Winey, K. I.; Laurer, J. H.; Kirkmeyer, B. P. *Macromolecules* **1999**, *33*, 507.
(7) Yarusso, D. J.; Cooper, S. L. *Macromolecules* **1983**, *16*, 1871.
(8) Zhou, N. C.; Chan, C. D.; Winey, K. I. *Macromolecules* **2008**, *41*, 6134.
(9) Kim, J.-S.; Yoshikawa, K.; Eisenberg, A. *Macromolecules* **1994**, *27*, 6347–6357.
(10) Tant, M. R.; Venkateshwaran, L. N.; Song, J. H.; Subramanian, R.; Wilkes, G. L.; Charlier, P.; Jérôme, R. *Polymer* **1992**, *33*, 1347–1358.
(11) Kirkmeyer, B. P.; Weiss, R. A.; Winey, K. I. *J. Polym. Sci., Part B: Polym. Phys.* **2001**, *39*, 477.
(12) Li, C.; Register, R. A.; Cooper, S. L. *Polymer* **1989**, *30*, 1227.
(13) O'Connell, E. M.; Root, T. W.; Cooper, S. L. *Macromolecules* **1995**, *28*, 3995.
(14) Spontak, R. J.; Williams, M. C.; Agard, D. A. *Polymer* **1988**, *29*, 387–395.
(15) Jinnai, H.; Nishikawa, Y.; Spontak, R. J.; Smith, S. D.; Agard, D. A.; Hashimoto, T. *Phys. Rev. Lett.* **2000**, *84*, 518.
(16) Drummy, L. F.; Wang, Y. C.; Schoenmakers, R.; May, K.; Jackson, M.; Koerner, H.; Farmer, B. L.; Mauryama, B.; Vaia, R. A. *Macromolecules* **2008**, *41*, 2135–2143.
(17) Ikeda, Y.; Katoh, A.; Shimanuki, J.; Kohjiya, S. *Macromol. Rapid Commun.* **2004**, *25*, 1186–1190.
(18) Jinnai, H.; Shinbori, Y.; Kitaoka, T.; Akutagawa, K.; Mashita, N.; Nishi, T. *Macromolecules* **2007**, *40*, 6758–6764.
(19) Jinnai, H.; Spontak, R. J. *Polymer* **2009**, *50*, 1067–1087.

(20) Jinnai, H.; Spontak, R. J.; Nishi, T. *Macromolecules* **2010**, *43*, 1675–1688.
(21) Loos, J.; Sourty, E.; Lu, K.; Freitag, B.; Tang, D.; Wall, D. *Nano Lett.* **2009**, *9*, 1704–1708.
(22) Lu, K.; Sourty, E.; Guerra, R.; Bar, G.; Loos, J. *Macromolecules* **2010**, *43*, 1444–1448.
(23) Midgley, P. A.; Weyland, M. *Ultramicroscopy* **2003**, *96*, 413–431.
(24) Akasaka, S.; Okamoto, T.; Osaka, T.; Matsushita, T.; Hasegawa, H. *Eur. Polym. J.* **2010**, *47*, 651–661.
(25) Sugimori, H.; Nishi, T.; Jinnai, H. *Macromolecules* **2005**, *38*, 10226–10233.
(26) Makowski, H. S.; Lundberg, R. D.; Singhal, G. H. US Patent 3 870 841, March 11, 1975 (assigned to Exxon Research and Engineering Co.).
(27) Dalmas, F.; Vonet, J.-F.; Randriamahefa, S.; Gaillet, C. *Macromol. Chem. Phys.* **2010**, *211*, 1765–1774.
(28) Heidari Mezerji, H.; Van den Broek, W.; Bals, S. *Ultramicroscopy* **2011**, *111*, 330–336.
(29) ImageJ homepage: http://rsbweb.nih.gov/ij/.
(30) Bolte, S.; Cordelières, F. P. *J. Microsc.* **2006**, *224*, 213–232.
(31) Atorngitjawat, P.; Runt, J. *Macromolecules* **2007**, *40*, 991–996.
(32) Vermogen, A.; Masenelli-Varlot, K.; Seguela, R.; Duchet-Rumeau, J.; Boucard, S.; Prele, P. *Macromolecules* **2005**, *38*, 9661.
(33) Pan, Y.; Xu, Y.; An, L.; Lu, H.; Yang, Y.; Chen, W.; Nutt, S. *Macromolecules* **2008**, *41*, 9245–9258.
(34) Kawase, N.; Kato, M.; Nishioka, H.; Jinnai, H. *Ultramicroscopy* **2007**, *107*, 8–15.
(35) Batra, A.; Cohen, C.; Kim, H.; Winey, K. I.; Ando, N.; Gruner, S. M. *Macromolecules* **2006**, *39*, 1630–1638.
(36) O'Connell, E. M.; Peiffer, D. G.; Root, T. W.; Cooper, S. L. *Macromolecules* **1996**, *29*, 2124–2130.
(37) Chu, B.; Wu, D. Q.; MacKnight, W. J.; Wu, C.; Phillips, J. C.; LeGrand, A.; Lantman, C. W.; Lundberg, R. D. *Macromolecules* **1988**, *21*, 523–525.